

## Ionic Strength-Controlled Virtual Area of Mesoporous Platinum Electrode

Hankil Boo,<sup>†,‡</sup> Sejin Park,<sup>†,‡</sup> Bonkyung Ku,<sup>†</sup> Yunmee Kim,<sup>†</sup> Jin Hyung Park,<sup>‡</sup> Hee Chan Kim,<sup>\*,‡</sup> and Taek Dong Chung<sup>\*,†</sup>

Department of Chemistry, Sungshin Women's University, 249-1 Dongsun-dong, Sungbuk-gu, Seoul 136-742, Korea, and Department of Biomedical Engineering, College of Medicine and Institute of Medical and Biological Engineering, Medical Research Center, Seoul National University, 28 Yongon-dong, Chongno-gu, Seoul 110-744, Korea

Received November 27, 2003; E-mail: chembud@sungshin.ac.kr; hckim@snu.ac.kr

Since it was first shown that a hexagonal liquid crystalline phase can be used as a template to fabricate mesoporous platinum (Pt) films by an electrochemical method,<sup>1</sup> mesoporous Pt has received much attention with regard to its potential applications. Corresponding research efforts have produced a number of impressive applications.<sup>2–4</sup> One of those accomplishments is the enzymeless glucose sensor.<sup>3</sup> The strategy involved exploiting the unusually large surface area of the mesoporous electrodes to selectively amplify the current due to the direct oxidation of glucose without an enzyme like glucose oxidase. Other examples than enzymeless glucose sensor include the amperometric enhancements of oxidation of methanol, hydrogen peroxide, and reduction of oxygen.<sup>4</sup> Most of such applications utilize the high roughness of mesoporous Pt.

However, the classical Gouy–Chapman theory<sup>5,6</sup> predicts that the geometric area enlarged by morphological porosity is not necessarily equivalent to the electrochemically active area of electrode. Theoretically, the effective area of a mesoporous electrode, which is available for electrochemical reaction, can be described as a function of two variables. One is the pore radius ( $r$ ), and the other is the characteristic thickness of the double layer, the so-called Debye length ( $\kappa^{-1}$ ).<sup>7</sup> It is convenient to think of an equi-potential line that is far from the electrode surface by  $\kappa^{-1}$ . In case of  $\kappa^{-1} < r$ , the equi-potential line is so close to the surface of the pores that the active area should be much larger than that of a flat electrode. On the other hand, when  $\kappa^{-1} > r$ , the pore is too narrow for the equi-potential line to follow the geometric surface as it is. Instead, the electrical double layer extends to outside the pores and no substantial potential drop occurs inside the pores.<sup>8</sup> As a result, a critical change in the shape of the electric double layer takes place in proximity to the surface of mesoporous electrodes when the diameter of pores falls down to nanometer scale, which are comparable with the thickness of the electrical double layer. The Gouy–Chapman theory states

$$\kappa = (3.29 \times 10^7) z C^*{}^{1/2} \quad (1)$$

where  $C^*$  is the bulk  $z:z$  electrolyte concentration in mol L<sup>-1</sup> and  $\kappa$  is given in cm<sup>-1</sup>.<sup>6</sup> It indicates that  $\kappa^{-1}$  decreases as the electrolyte concentration increases. As for the electrodes with the pores of several nanometers in diameter, the effective area may depend on the ionic strength. It is conceivable in such a system that the shape of the interface between the electrical double layer and the bulk solution phase shifts from the flat to the porous and vice versa as the concentration of electrolyte varies over a certain characteristic value, which is closely related to the pore diameter. Here, we experimentally demonstrate the novel phenomenon taking place on

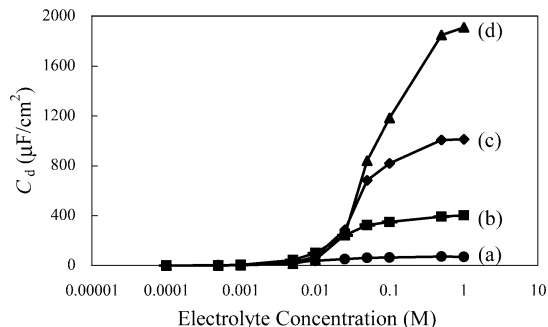


**Figure 1.** Differential capacitances of (a) flat (roughness factor 2.37) and (b–d) mesoporous Pt electrodes in various electrolyte concentrations at  $-0.5$  V versus Hg/Hg<sub>2</sub>SO<sub>4</sub>.  $C_d$ 's were calculated with respect to geometric area (flat electrode,  $3.14 \times 10^{-2}$  cm<sup>2</sup>; porous electrode,  $7.85 \times 10^{-3}$  cm<sup>2</sup>). The charges for Pt deposition and roughness factors of mesoporous Pt electrodes are (b) 5 mC and 29.1, (c) 10 mC and 65.1, and (d) 25 mC and 158, respectively.

a mesoporous structure and show a unique application, which is the dramatic control of faradaic current density by adjusting ionic strength only.

Differential capacitance ( $C_d$ )<sup>9,10</sup> is a good experimental indicator to probe the change in effective electrode area. The electrode and electrolyte for the measurements were mesoporous Pt (pore diameter of 2.5 nm)<sup>1–3</sup> and NaF,<sup>6,11</sup> respectively. The roughness factors of Pt electrodes, with constant pore size and various pore lengths,<sup>3,4</sup> were controlled by charge passed for electrodeposition and were determined by cyclic voltammetry through the charge for hydrogen adsorption (Supporting Information).<sup>12</sup> Figure 1 shows the  $C_d$ 's of a flat and three mesoporous electrodes. The  $C_d$  values are almost the same and increase very slowly in the range of the electrolyte concentration below  $1 \times 10^{-2}$  M. In these diluted ionic solutions, thick electrical double layers are expectedly formed along the geometric surface of electrodes. On the other hand, the  $C_d$ 's of mesoporous Pt electrodes rise precipitously in the concentration higher than  $1 \times 10^{-2}$  M, while that of the flat Pt electrode keeps growing at a slow rate. The steep increase of  $C_d$ 's begins at between  $1 \times 10^{-2}$  and  $1 \times 10^{-1}$  M.<sup>13</sup>

Equation 1 says that  $\kappa^{-1}$  is theoretically equal to  $r$  (1.25 nm in this study) when the electrolyte concentration is  $5.9 \times 10^{-2}$  M. This agrees well with the transition points of  $C_d$ 's shown in Figure 1. The consistency between the experimental results and the theoretical prediction shows that the mesoporous structure of the electrode surface can make it possible to induce the unusual electrochemical event that has not been realized before, discrepancy between the shapes of the geometric surface and the apparent electrical double layer. Figure 2 shows the schematic sketch of how the electric double layer changes as the ionic strength varies. At a low electrolyte concentration, the equi-potential line of  $\kappa^{-1}$  in the

<sup>†</sup> Sungshin Women's University.

<sup>‡</sup> Seoul National University.

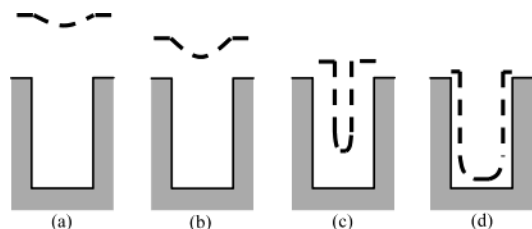


**Figure 2.** Schematic diagram displaying the shapes of the electrical double layers that depend on the electrolyte concentration: (a) 1 mM, (b) 10 mM, (c) 100 mM, and (d) 1000 mM.

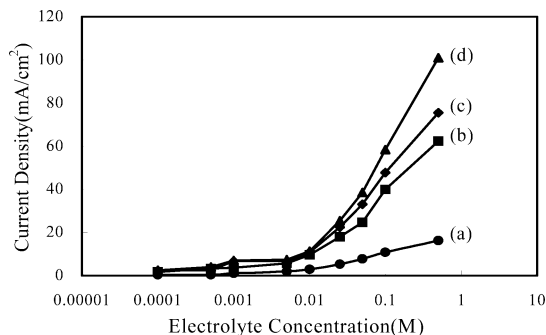


**Figure 3.** The results of chronoamperometry of  $O_2$  reduction at (a) flat and (b–d) mesoporous Pt electrodes at various electrolyte concentrations. The concentration of  $O_2$  is about 1 mM. Step potential is  $-0.75$  V versus  $Hg/Hg_2SO_4$ . Sampling time is 11 ms. The roughness factors of mesoporous Pt electrodes are (a) 2.37, (b) 29.1, (c) 65.1, and (d) 158.

electrical double layer on the mesoporous surface looks more like that of the flat than of the porous as shown Figure 2a and b. On the other hand, higher electrolyte concentration makes the electrical double layer thinner and closer to the walls of the nanopores as seen in Figure 2c and d. As a result, the area of the interface between the electrical double layer and the bulk solution phase, on which the potential gradient is steep enough to induce faradaic reaction, expands remarkably eventually up to the roughness factor (Supporting Information).

This phenomenon can lend itself to the control of faradaic current density by altering supporting electrolyte concentration. The electrochemical reduction of dioxygen is one of the good examples that show the functional applicability of the unique behavior on the mesoporous Pt electrodes. The electrochemical reduction of aqueous dioxygen on a flat Pt surface is hardly diffusion-controlled.<sup>14</sup> Figure 3 shows the current density for dioxygen reduction at a flat and mesoporous Pt electrodes in various electrolyte concentrations. The current density from the flat Pt grows gradually as the electrolyte concentration increases. The porous electrodes provide a little larger current density at electrolyte concentrations below  $1 \times 10^{-2}$  M than does the flat one. This is presumably attributed to the macroscopic roughness factor of mesoporous Pt. Nevertheless, no significant difference is observed between the data from the flat and the mesoporous for dilute ionic solutions by and large. Above the electrolyte concentration of  $1 \times 10^{-2}$  M, the current density begins to climb steeply. The trend looks similar to that of  $C_d$  shown in Figure 1. The larger area of the Pt surface participating in the electrochemical reduction obviously brings about higher current as the inner walls of the pores as well as the outermost surface of mesoporous Pt participate in the faradaic reaction. As the ionic strength increases, the current density reaches such a high region that the electrochemical system

apparently becomes more like the diffusion-controlled reduction of dioxygen. This result indicates that the electrolyte concentration can be a key variable governing the rate of electrochemical reaction on a mesoporous Pt electrode.

In conclusion, we have shown that the interface between the electrical double layer and the bulk solution phase on mesoporous electrodes depends on the ionic strength and the faradaic current at mesoporous electrode can be critically controlled by electrolyte concentration. The phenomenon addressed in this study suggests many implications in terms of practical applications as well as fundamental electrochemistry of nanoporous electrodes, for instance, understanding the electrochemical behavior on the nanoporous electrodes applied for fuel cells and nanochannels that open and shut the electroosmotic flow depending on ionic strength for microfluidic chips.

**Acknowledgment.** This work was supported by a Korea Research Foundation Grant (KRF-2002-C00066).

**Supporting Information Available:** Experimental details. Cyclic voltammograms, chronoamperometry, and differential capacitances measured (PDF). This material is available free of charge via the Internet at <http://pubs.acs.org>.

## References

- (1) Attard, G. S.; Bartlett, P. N.; Coleman, N. R. B.; Elliott, J. M.; Owen, J. R.; Wang, J. H. *Science* **1997**, *278*, 838–840.
- (2) (a) Bartlett, P. N.; Baumberg, J. J.; Birkin, P. R.; Ghanem, M. A.; Netti, M. C. *Chem. Mater.* **2002**, *14*, 2199–2208. (b) Elliott, J. M.; Birkin, P. R.; Bartlett, P. N.; Attard, G. S. *Langmuir* **1999**, *15*, 7411–7415. (c) Gollas, B.; Elliott, J. M.; Bartlett, P. N. *Electrochim. Acta* **2000**, *45*, 3711–3724. (d) Nandhakumar, I.; Elliott, J. M.; Attard, G. S. *Chem. Mater.* **2001**, *13*, 3840–3842. (e) Nelson, P. A.; Elliott, J. M.; Attard, G. S.; Owen, J. R. *Chem. Mater.* **2002**, *14*, 524–529. (f) Yang, K.-L.; Yiacoumi, S.; Tsouris, C. *Nano Lett.* **2002**, *2*, 1433–1437. (g) Elliott, J. M.; Owen, J. R. *Phys. Chem. Chem. Phys.* **2000**, *2*, 5653–5659.
- (3) Park, S.; Chung, T. D.; Kim, H. C. *Anal. Chem.* **2003**, *75*, 3046–3049.
- (4) (a) Evans, S. A. G.; Elliott, J. M.; Andrews, L. M.; Bartlett, P. N.; Doyle, P. J.; Denuault, G. *Anal. Chem.* **2002**, *74*, 1322–1326. (b) Kucernak, A.; Jiang, J. *Chem. Eng. J.* **2003**, *93*, 81–90. (c) Birkin, P. R.; Elliott, J. M.; Watson, Y. E. *Chem. Commun.* **2000**, 1693–1694.
- (5) (a) Grahame, D. C. *Chem. Rev.* **1947**, *41*, 441–501. (b) Grahame, D. C. *J. Am. Chem. Soc.* **1954**, *76*, 4819–4823.
- (6) Bard, A. J.; Faulkner, L. R. *Electrochemical Methods: Fundamentals and Applications*, 2nd ed.; John Wiley & Sons: New York, 2001; Chapter 13.
- (7) (a) Kemery, P. J.; Steehler, J. K.; Bohn, P. W. *Langmuir* **1998**, *14*, 2884–2889. (b) Kuo, T.-C.; Sloan, L. A.; Sweedler, J. V.; Bohn, P. W. *Langmuir* **2001**, *17*, 6298–6303.
- (8) Corry, B.; Kuyucak, S.; Chung, S. H. *Chem. Phys. Lett.* **2000**, *320*, 35–41.
- (9) (a) Gileadi, E.; Argade, S. D.; Bockris, J. O'M. *J. Phys. Chem.* **1966**, *70*, 2044–2046. (b) Bockris, J. O'M.; Khan, S. U. M. *Surface Electrochemistry: A Molecular Level Approach*; Plenum Press: New York, 1993; Chapter 2.
- (10) (a) Jović, V. D.; Jović, B. M. *J. Electroanal. Chem.* **2003**, *541*, 1–11. (b) Lust, E.; Nurk, G.; Jänes, A.; Arulepp, M.; Nigu, P.; Möller, P.; Kallip, S.; Sammelselg, V. *J. Solid State Electrochem.* **2003**, *7*, 91–105. (c) Pajkossy, T.; Kolb, D. M. *Electrochem. Commun.* **2003**, *5*, 283–285. (d) Pajkossy, T.; Kolb, D. M. *Electrochim. Acta* **2001**, *46*, 3063–3071.
- (11) Valette, G. *J. Electroanal. Chem.* **1982**, *138*, 37–54.
- (12) Sawyer, D. T.; Sobkowiak, A.; Roberts, J. L., Jr. *Electrochemistry for Chemists*; John Wiley & Sons: New York, 1995; pp 216–219.
- (13) The  $C_d$ 's in Figure 1 were measured at near the potential of zero charge ( $E_z$ ) (see ref 9). Yet these phenomena were observed in the wide range of potential, even far from  $E_z$ . The Gouy–Chapman–Stern (GCS) theory tells the relation of  $1/C_d = 1/C_H + 1/C_D$ , where  $C_H$  and  $C_D$  are the capacitance due to Helmholtz layer and the diffuse capacitance, respectively.  $C_d$  significantly depends on  $C_D$  at the mesoporous electrode unlike the flat electrode because  $C_H$  is remarkably enlarged by porous structure.  $C_D$  is a function of electrolyte concentration, while  $C_H$  is not.
- (14) Bockris, J. O'M.; Khan, S. U. M. *Surface Electrochemistry: A Molecular Level Approach*; Plenum Press: New York, 1993; Chapter 3.

JA0398316